THERAPEUTIC ADVANCES in
Medical Oncology

Original Research

Ferroptosis-related genes as prognostic markers for survival and immunotherapy in triple-negative breast cancer: analysis of public databases and a single institution

Ther Adv Med Oncol

2025, Vol. 17: 1–13

DOI: 10.1177/17588359251322291

Yizhao Xie*, Zhonghua Tao*, Biyun Wang, Yannan Zhao, Xinyu Chen, Bin Li, Jinyan Wang, Guangliang Chen* and Xichun Hu*

Abstract

Background: Ferroptosis plays a vital role in cancer development and treatment. The relationship between ferroptosis-related genes and breast cancer prognosis, as well as immunotherapy outcomes, remains unknown.

Objectives: To evaluate the prognostic value of ferroptosis-related genes in breast cancer.

Methods: We conducted differential expressions and prognostic analysis for ferroptosis-related genes on public databases and breast cancer patients in our center and analyzed their predictive value for immunotherapy of breast cancer patients.

Results: We identified prognostic ferroptosis-related genes, constructed a nomogram, and validated key genes using patient data from our center. We also investigated ferroptosis-related genes significantly associated with immune infiltration and identified *FTH1* as a promising biomarker for triple-negative breast cancer immunotherapy.

Conclusion: Ferroptosis-related genes had potential prognostic value and predictive value for breast cancer immunotherapy.

Keywords: breast cancer, ferroptosis, immunotherapy, prognosis

Received: 25 October 2024; revised manuscript accepted: 5 February 2025.

Correspondence to:
Xichun Hu
Guangliang Chen
Department of Medical Oncology, Fudan University Shanghai Cancer Center, 270 Dongan Road, 200032, Shanghai, China

Department of Oncology, Shanghai Medical College, Fudan University, Shanghai, China
huxichun2017@163.com
guangliang_chen@fudan.edu.cn

Yizhao Xie
Zhonghua Tao
Biyun Wang
Yannan Zhao
Xinyu Chen
Bin Li
Jinyan Wang
Department of Medical Oncology, Fudan University Shanghai Cancer Center, 200032, Shanghai, China

Department of Oncology, Shanghai Medical College, Fudan University, Shanghai, China

*These authors contributed equally.

Introduction

Female breast cancer is the most common cancer type worldwide, causing 2.3 million new cases and 690 thousand deaths each year.[1] Triple-negative breast cancer (TNBC) is defined as the absence of estrogen receptor, progesterone receptor, and human epidermal growth factor receptor-2, which comprises 15%–20% of all cases.[2] TNBC shows a more malignant biological behavior, higher recurrence rate, fewer treatment options, and worse prognosis compared to other subtypes.[3,4] Due to few therapy options and relatively short overall survival (OS), more accurate prognostic factors and treatment options are warranted.

Ferroptosis, a novel form of regulated cell death driven by excessive lipid peroxidation, has been reported to reflect multiple pathways in cancer pathogenesis and development.[1,5] Experimental molecules such as erastin and approved drugs such as sulfasalazine (for ulcerative colitis) could induce ferroptosis through inhibiting system XC-L-glutathione reduced-glutathione peroxidase 4 (*GPX4*) pathway.[6] A more recent study found that poly (ADP-ribose) polymerases inhibitor induces ferroptosis in ovarian cancer through inhibition of SLC7A11 (*xCT*) in a P53-dependent manner.[7] Furthermore, anti-programmed death ligand 1 (PD-L1) antibodies were reported to promote lipid peroxidation-dependent ferroptosis in tumor cells and had synergistic actions in tumor inhibition when combined with ferroptosis activators such as erastin.[8] However, few studies explored the prognostic and immunotherapy

predictive value of ferroptosis-related genes in breast cancer patients.

Although chemotherapy remains the cornerstone in metastatic TNBC (mTNBC), immunotherapy has recently shown exciting results. A phase III IMpassion130 study enrolled 902 metastatic or inoperable TNBC patients and randomized them into atezolizumab or placebo plus nab-paclitaxel. The results showed significantly improved progression-free survival (PFS) in the atezolizumab group.[9] However, the phase III IMpassion131 study showed that atezolizumab combined with paclitaxel did not significantly improve the survival outcome in PD-L1-positive patients.[10] The KEYNOTE-355 study compared pembrolizumab or placebo plus chemotherapy in first-line treatment of mTNBC and indicated prolonged PFS in PD-L1-positive patients or patients with a combined positive score of greater than 10.[11] Although immunotherapy provides a great opportunity for patients, controversial results in different studies urge us to find more efficient biomarkers and prognostic factors to identify proper candidates for immunotherapy.

Thus, in this study, we explored the differential expression, prognostic value, and immunotherapy prediction of ferroptosis-related genes in breast cancer patients both in public databases and in our center. These findings could deepen our understanding of ferroptosis in breast cancer and uncover novel biomarkers for immunotherapy of breast cancer.

Methods

Gene expression, prognostic effect, and functional analysis in a public database

The mRNA expression data of normal and tumor tissues, as well as clinical outcomes of patients with breast cancer, were obtained from the GEO database: GSE93601[12] (https://www.ncbi.nlm.nih.gov/geo) and The Cancer Genome Atlas (TCGA) database: TCGA-BRCA (https://www.cancer.gov/tcga/). All data were normalized via log2-scale transformation to ensure standardization. Differential expression was analyzed by the "limma" package in R (version 4.0.2). Survival analysis was performed by "survival" package. Univariate and multivariate Cox regression models were used to identify the survival-related ferroptosis-related genes. A total of 149 ferroptosis-related genes, including drivers, suppressors, and markers, were obtained from the FerrDb database (http://www.zhounan.org/ferrdb/).[13] Functional analysis and network production were performed on Metascape Online (https://metascape.org/gp/index.html#/main/step1).[14]

Nomogram construction

A nomogram was used to collect the prognostic factors and visualize the risk model for the calculation of the probability of 1, 3, and 5-year OS.[15] The calibration curve was mapped to evaluate the consistency between predicted and observed probability. The R packages "rms" and "survival" were used in the construction of the nomogram and calibration curves. In this nomogram, we could simply calculate the OS probability by adding up scores of each variable and locating this sum on the line of "total points." Bootstrap self-sampling method and graphic calibration method were used to validate our model.

Human breast cancer tissue specimens

A set of tissue microarrays (TMAs) including 258 breast cancer patients was obtained from their first radical surgery with no prior systemic treatment from 2010 to 2020.

Patient data were collected from an electronic medical records system. Resected specimens were macroscopically examined to confirm the location and size of a tumor. For histology use, the specimens were fixed in 10% (v/v) formalin and processed for paraffin embedding. The Ethics Committee and Institutional Review Boards at Fudan University Shanghai Cancer Center approved this study for clinical investigation. All of the patients signed written informed consent forms before the study.

Immunohistochemistry

The primary antibodies *SLC7A11/xCT* (26864-1-AP; Proteintech, Wuhan, China, 1:200), *ALOX12* (ab211506; Abcam, Cambridge UK, 1:50), *GPX4* (67763-1-Ig; Proteintech, 1:100), and *ACSL4* (22401-1-AP; Proteintech, 1:150) were used and incubated at 4°C overnight. TMA was scanned by Nikon E100 and processed through Nikon DS-U3 (Nikon, Tokyo, Japan) according to the manufacturer's instructions.

Staining score was evaluated by stain intensity and the percent of positive cells, each patient was scored 0, 1, 2, or 3. Patients with 0 or 1 score were defined as low expression and 2 or 3 as high expression.

Immune infiltration analysis

RNAseq data were extracted from the TCGA-BRCA database and a correlation analysis was performed between *FTH1* and immune infiltration matrix data. Using the ssGSEA algorithm provided in the R package GSVA1, the immune infiltration of 24 types of immune cells based on cloud data was performed.[16] Alternatively, the R package ESTIMATE was used to calculate the corresponding stromal and immune scores.[17] The analysis results were visualized using lollipop plots or violin plots with the ggplot2 package.

Immunotherapy cohort

A total of 12 patients with histologically confirmed mTNBC disease who used immunotherapy (PD-1/PD-L1 antibody)-based treatment as first-line treatment at Fudan University Shanghai Cancer Center were enrolled in our study.

Immunofluorescence

The immunofluorescence method is basically performed as before.[18] Briefly, after deparaffinization and antigen retrieval and blocking, incubate it overnight in primary antibody and 40 min in secondary antibody, washing, and TSA treatment before adding second primary antibody and second secondary antibody. Then stain it with DAPI before imaging.

Statistical analysis

The study results are presented as mean ± standard deviation for three independent experiments. Student's *t*-test was used for comparison between groups. OS and recurrence-free survival (RFS) curves were conducted using Kaplan–Meier analyses and compared using the log-rank test. All statistical analyses were performed using the GraphPad Prism® 8.0 software (GraphPad Software, Boston, USA), R software (version 4.0.2), or SPSS (version 23.0, IBM, Chicago, USA). $p < 0.05$ (two-sided) was considered statistically significant. The reporting of this study conforms to the TRIPOD statement[19] (Supplemental File 3).

Results

Differentially expressed ferroptosis-related genes in breast cancer

We first screened differential genes of cancer tissue and normal tissue from both the TCGA-BRCA database and the GEO: GSE93601 database. As a result, 1265 dysregulated genes in the GEO database and 4966 dysregulated genes in the TCGA database were found (Figure 1(a)). We then intersected these dysregulated genes with ferroptosis-related genes obtained from the FerrDb database (Table S1) and showed them with a Venn diagram (Figure 1(b)). A total of 96 differentially expressed ferroptosis-related genes were identified (Table S2).

To explore the relevant pathways of ferroptosis signatures in breast cancer, we performed Gene Ontology (GO) and Kyoto Encyclopedia of Genes and Genomes (KEGG) analysis using Metascape Online (Figure 1(c) and (d)). The results of GO analysis showed that these differential genes were enriched in ferroptosis, response to stress, and nutrient levels. Similarly, the KEGG analysis revealed pathway enrichment in ferroptosis, response to stimuli, and nutrient levels. Furthermore, we explored the expression levels of key ferroptosis-related genes in the TCGA-BRCA database and found most ferroptosis suppressors (e.g., *SLC7A11, FTH1*) are upregulated in breast cancer tissue compared to normal tissue, while most ferroptosis promoters (e.g., *ACSL4, ALOX12*) are downregulated (Figure 1(e)). These findings indicated that ferroptosis might play an important role in breast cancer.

Prognostic value of ferroptosis-related genes in breast cancer

To further assess the prognostic value of ferroptosis-related genes in breast cancer patients, we conducted Cox regression analysis and showed in Kaplan–Meier method using mRNA expression data and patients' survival information in the TCGA database. We found that six typical ferroptosis-related genes were associated with breast cancer prognosis: *SLC7A11*, *TFRC*, *FTH1*, *ALOX12*, *HSBP1*, and *CBS* (Figure 2(a)). Multivariate Cox regression revealed *ALOX12* as an independent prognostic factor (adjusted hazard ratio (HR) 0.671, 95% confidence interval (CI) 0.486–0.927, $p = 0.015$). Moreover, since TNBC showed more severe biological behavior

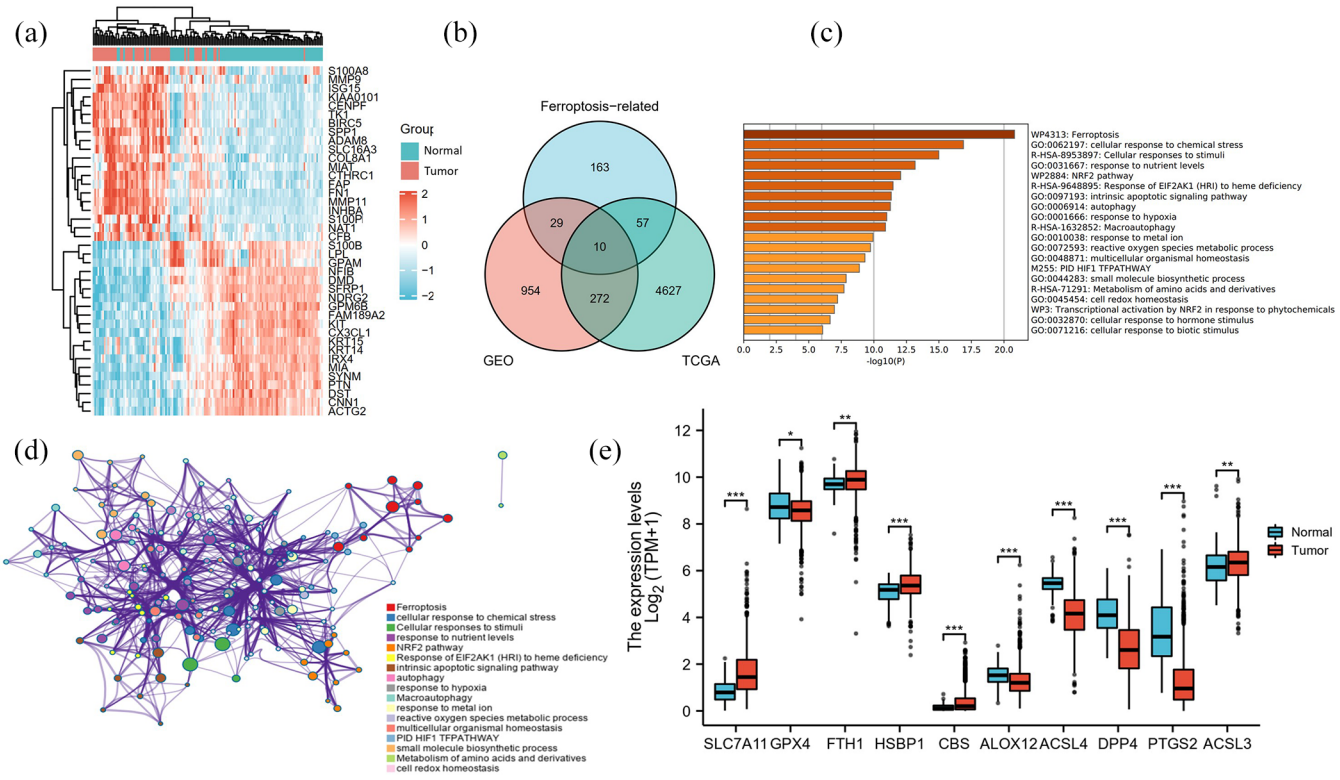

Figure 1. Differentially expressed ferroptosis-related genes in breast cancer. (a) Expression profiles of genes in normal and tumor samples in GSE93601. Genes were ranked according to their expression. The red color and blue color represent high and low expression. (b) Venn diagram of the differentially expressed genes and ferroptosis-related genes. (c, d) GO and KEGG analysis based on the Metascape Online. (e) Direct expression of differential genes using the TCGA-BRCA database.
GO, Gene Ontology; KEGG, Kyoto Encyclopedia of Genes and Genomes; TCGA, The Cancer Genome Atlas.

and poorer outcomes, we analyzed these genes in TNBC separately. The results confirmed the prognostic value of ferroptosis-related genes in TNBC patients (Figure 2(b)).

Construction of nomogram

Since multivariate analysis showed *ALOX12* as a predictive factor, we further used a nomogram to combine *ALOX12* with the basic characteristics of patients for survival prediction (Figure 3(a)).

We used two methods to validate our model. The concordance index (C-index) using the Bootstrap Self-sampling method, which could estimate the discrimination ability of the nomogram, was 0.730 (0.703–0.757). Furthermore, we performed graphic calibration method analysis and it also showed high accordance between predicted survival and actual survival both in 3-year OS and 5-year OS (Figure 3(b)).

Prognostic value of SLC7A11 and ALOX12 in our center

To further demonstrate the prognostic value of ferroptosis-related genes and their relations with adipocytes, we performed immunohistochemistry (IHC) tests for breast cancer patients in our center. A total of 258 breast cancer patients with tumor tissue array and complete medical records were enrolled and analyzed at Fudan University Shanghai Cancer Center (FUSCC). IHC staining was scored 0, 1, 2, and 3 according to stain intensity, and scores of 2 and 3 were defined as high expression. Baseline patient characteristics between two treatment groups divided by *SLC7A11* and *ALOX12* expression are summarized in Tables 1 and 2. No significant difference was observed in median age, T stage, and molecular types between high and low expression of both groups. *ALOX12* high or *SLC7A11* low patients had lower N stage and less vascular invasion. Survival analysis showed a significantly improved RFS in *ALOX12*-low patients compared to

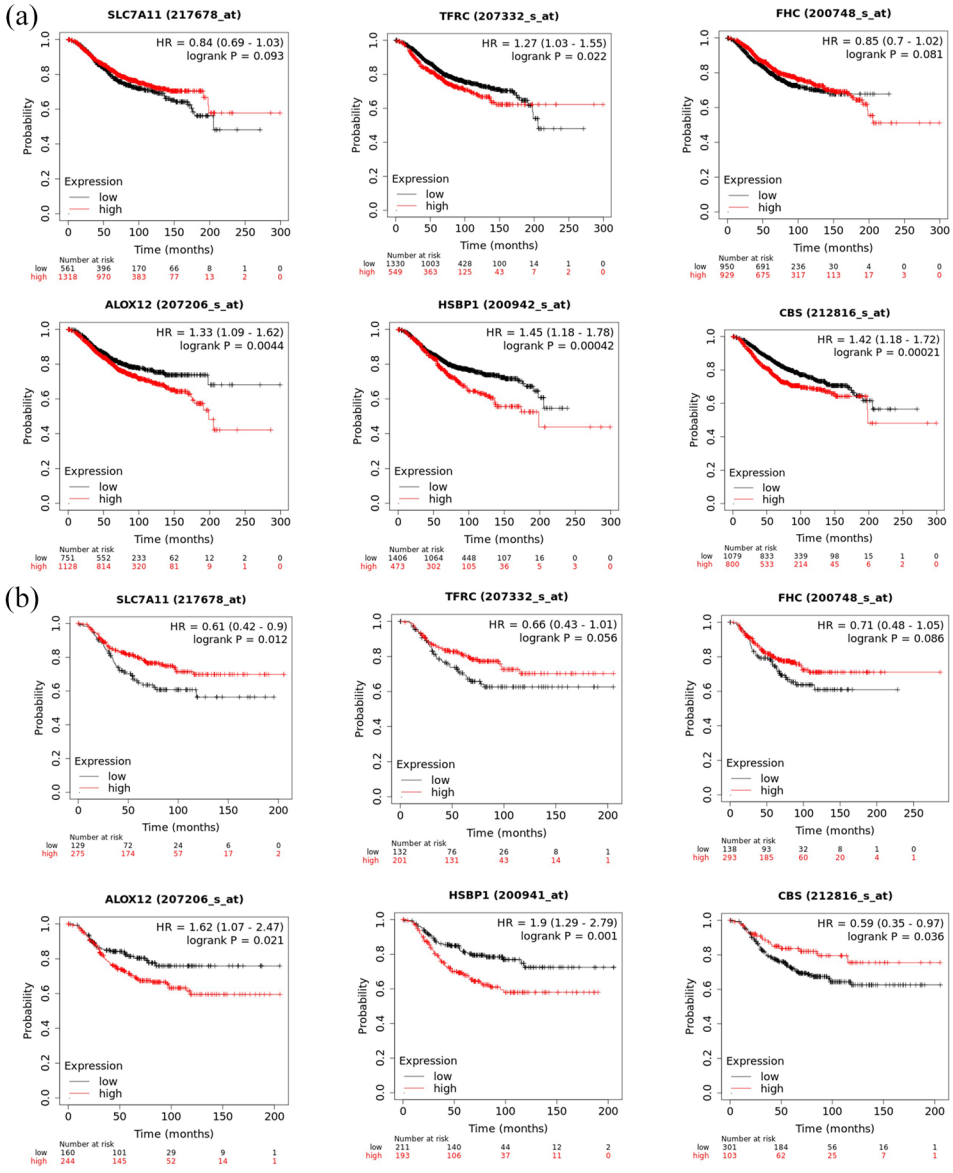

Figure 2. Ferroptosis-related genes predict the overall survival of breast cancer. (a) Kaplan–Meier plots show the ferroptosis-related genes with prognostic value in all breast cancer patients. (b) Kaplan–Meier plots show the ferroptosis-related genes with prognostic value in TNBC patients.
TNBC, triple-negative breast cancer.

ALOX12-high patients in all patients (Figure 4(a)) and TNBC subtype (Figure 4(b)).

Similarly, *SLC7A11*-high patients had a longer RFS compared to *SLC7A11*-low patients (Figure 4(c)), and a trend of predicting the TNBC subtype was observed (Figure 4(d)). Furthermore, we found that *ALOX12*-high and *SLC7A11*-low patients had significantly higher BMI scores (Figure 4(e) and (f)). Representative *ALOX12* (Figure 4(g)) and *SLC7A11* (Figure 4(h)) IHC figures were shown. These findings further suggested a meaningful prognostic value of *SLC7A11* and *ALOX12* and a close relation between fat tissue and ferroptosis in breast cancer patients.

FTH1 could predict immunotherapy outcomes of TNBC patients

We further evaluated ferroptosis-related genes and breast cancer immune infiltration.

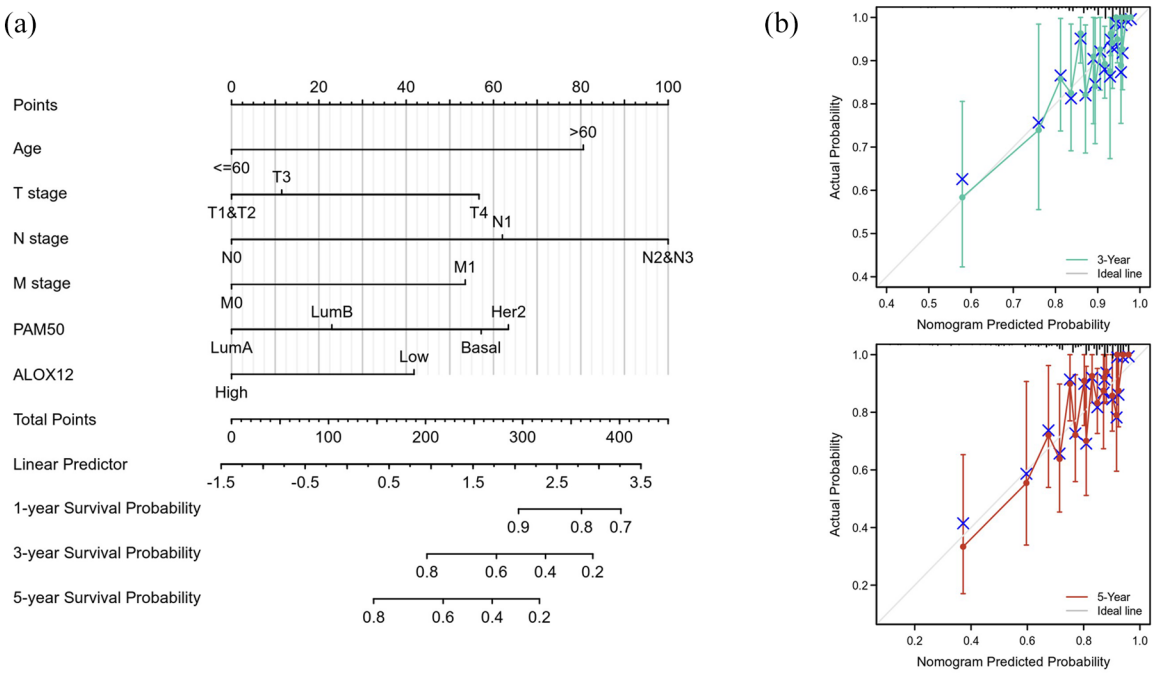

Figure 3. Nomogram for predicting 1-year, 3-year, and 5-year OS for breast cancer patients. (a) To calculate survival probability, locate points of patient variables, add points, and locate the sum on the total points line. (b) Calibration curves for the probability of 3-year and 5-year OS.
OS, overall survival.

We found that patients with high *FTH1* expression had significantly higher levels of immune infiltration. The enriched immune cells included major immune effector cells such as NK cells and CD8+ T cells (Figure 5(a)). In addition, patients with high *FTH1* expression had higher immune infiltration scores (Figure 5(b)). Subsequently, we included 12 TNBC patients from our center who received first-line immunotherapy for advanced disease and had available paraffin-embedded tissue sections. Immunofluorescence staining for *FTH1* and PD-L1 was performed, with baseline information provided in Table 3. The results showed a significant positive correlation between *FTH1* and PD-L1 expression (Figure 5(c)). Patients with high *FTH1* expression had a significantly better median PFS compared to those with low *FTH1* expression (12.4 vs 5.4 months, $p = 0.005$), and patients with high PD-L1 expression had a significantly better median PFS compared to those with low PD-L1 expression (12.4 vs 6.8 months, $p = 0.016$; Figure 5(d) and (e)). Multivariate analysis indicated that high *FTH1* expression was an independent predictor of immunotherapy efficacy (HR = 0.052, 95% CI 0.006–0.478). Figure 5(f) shows immunofluorescence images of two typical patients, patient I had a PFS of 12 months and patient II had a PFS of 6 months.

Discussion

As a newly discovered form of programmed cell death, ferroptosis plays a more and more important role in tumor treatment and therapy resistance. However, cancer cells could use multiple ways to escape from ferroptosis. We previously found the protection value of adipocytes against breast cancer ferroptosis.[20] The present study further explored the prognostic value of ferroptosis-related genes on breast cancer, as well as the relationship between adipocytes and ferroptosis using public database and data from our center. Moreover, a novel combination strategy was figured out to overcome protection against breast cancer ferroptosis.

At first, breast cancer was considered less sensitive to ferroptosis in terms of limited ferroptosis inducers.[21] With the increasing knowledge of

Table 1. Baseline patient characteristics between two treatment groups divided by *ALOX12* expression.

Characteristics	ALOX12 low *N* = 124 *n* (%)	ALOX12 high *N* = 134 *n* (%)	*p* Values
Median age	51	52	0.75
(Range)	(24–77)	(27–82)	
T stage			
1	28 (23)	32 (24)	0.88
2	91 (74)	98 (73)	
⩾3	5 (4)	4 (3)	
N stage			
0	87 (70)	66 (49)	0.003
1	20 (16)	33 (25)	
⩾2	17 (14)	35 (26)	
Vascular invasion			
Yes	35 (28)	66 (49)	0.001
No	89 (72)	68 (51)	
Molecular types			
Luminal	39 (31)	41 (30)	0.97
HER-2	33 (27)	35 (26)	
TNBC	52 (42)	58 (43)	
Median BMI	35	37	0.012
(Range)	(25–47)	(27–55)	

HER-2, human epidermal growth factor receptor-2; TNBC, triple-negative breast cancer.

ferroptosis, more and more evidence indicates that ferroptosis participates in not only the inhibition of breast cancer growth but also the synergistic anticancer effect together with targeted therapy, especially for TNBC.[22,23] Thus, investigation into ferroptosis protection could help us better understand the underlying mechanism of development, metastasis, and treatment response of breast cancer. We identify 96 ferroptosis-related genes differentially expressed in breast cancer and find six genes as predictors for breast cancer prognosis both in all patients and the TNBC subgroup, which on one hand adds evidence to support a link between ferroptosis and breast cancer and on the other hand give a hint for future studies.

ALOX12 catalyzes the production of lipid mediator which mediates cellular PUFA levels to regulate ferroptosis levels.[24] It is also reported that *ALOX12* is required for a distinct ferroptosis pathway of p53-mediated tumor suppression.[25] We found *ALOX12* as an independent predictor of OS in breast cancer patients and established a nomogram figure to visualize the risks for convenient use. The C-index of the nomogram is 0.7, which could be attributed to other genomic influences on prognosis not included in the

Table 2. Baseline patient characteristics between two treatment groups divided by *SLC7A11* expression.

Characteristics	SLC7A11 low *N* = 137 *n* (%)	SLC7A11 high *N* = 121 *n* (%)	*p* Values
Median age	51	52	0.52
(Range)	(27–82)	(24–77)	
T stage			
1	32 (23)	28 (23)	0.98
2	100 (73)	89 (74)	
⩾3	5 (4)	4 (3)	
N stage			
0	70 (51)	83 (68)	0.01
1	31 (23)	22 (18)	
⩾2	36 (26)	16 (12)	
Vascular invasion			
Yes	66 (48)	35 (29)	0.002
No	71 (52)	86 (71)	
Molecular types			
Luminal	40 (29)	40 (33)	0.51
HER-2	34 (25)	34 (28)	
TNBC	63 (46)	47 (39)	
Median BMI	37	36	0.026
(Range)	(27–55)	(25–47)	

HER-2, human epidermal growth factor receptor-2; TNBC, triple-negative breast cancer.

nomogram. Similarly, *ALOX12* was found to predict treatment response and prognosis of colorectal cancer.[26] Moreover, IHC staining in our center showed predictive value of *ALOX12* and *xCT* in RFS of breast cancer patients. We also found that patients with different expressions of *ALOX12* and xCT had differences in N staging and vascular invasion, further suggesting that these genes may be involved in the regulation of breast cancer invasion and metastasis. As far as we know, this is the first study reporting the prognostic value of *ALOX12* and *xCT* both in medical centers and databases of breast cancer patients.

FTH1 is an important component of ferritin, responsible for storing cytoplasmic iron and exerting cellular antioxidant effects by sequestering oxidative active iron.[27] Both in vitro and in vivo experiments have confirmed that ferritin, as a key regulator of ferroptosis, can mediate cell sensitivity to ferroptosis.[28,29] Our exploration suggests that *FTH1* may be related to immune infiltration in breast cancer. We further proved *FTH1* expression as an effective predictor for immunotherapy outcome of TNBC patients. The potential mechanism might be the upregulation of iron metabolism by *FTH1* causing a reduction of oxidative stress and ferroptosis of the immune

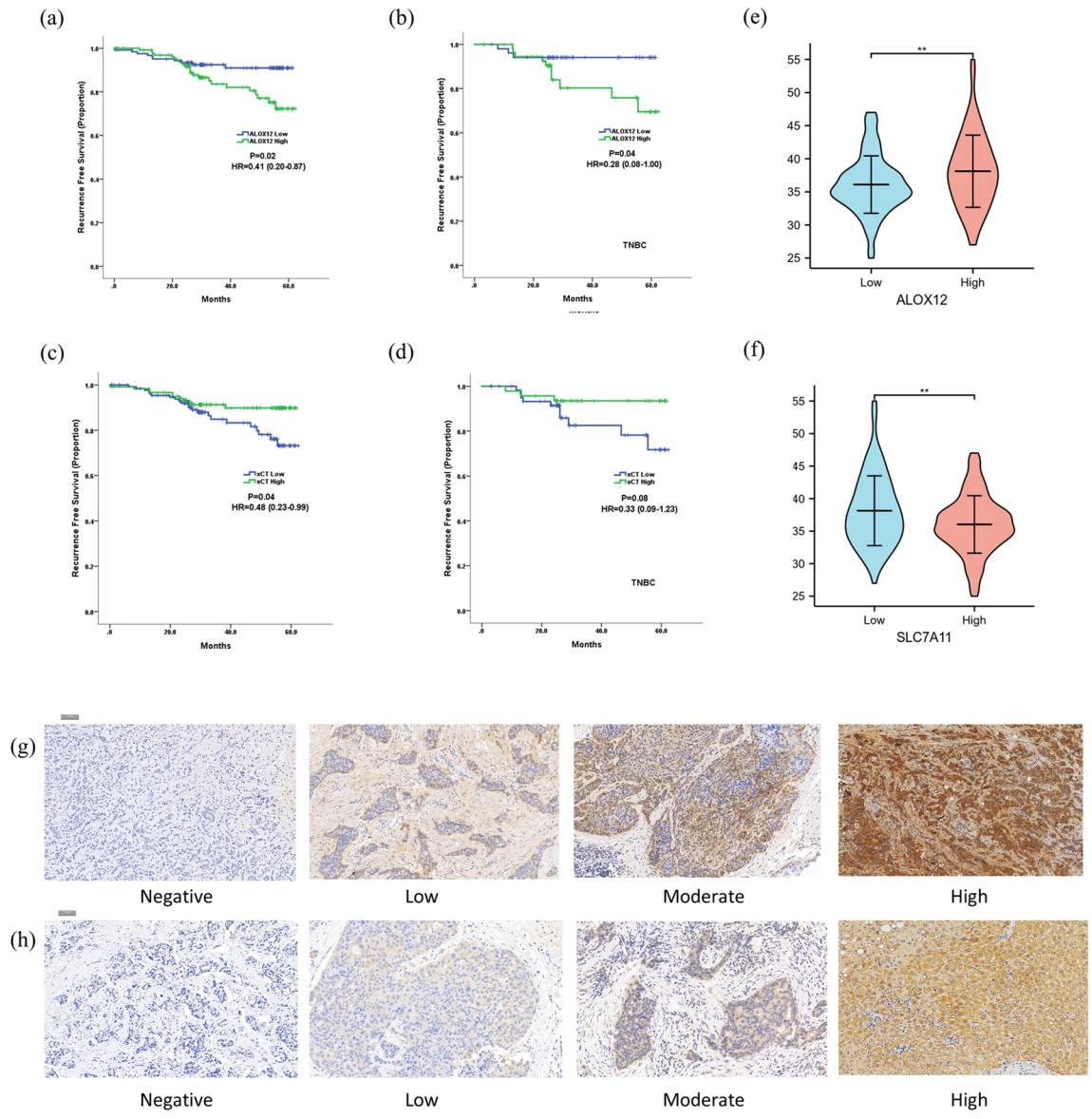

Figure 4. Prognostic value of *SLC7A11* and *ALOX12* in FUSCC. (a) Kaplan–Meier curves for RFS divided by *ALOX12* expression in all patients. (b) Kaplan–Meier curves for RFS divided by *ALOX12* expression in TNBC patients. (c) Kaplan–Meier curves for RFS divided by *SLC7A11* expression in all patients. (d) Kaplan–Meier curves for RFS divided by *SLC7A11* expression in TNBC patients. (e) Violin plot of BMI score divided by *ALOX12* expression. (f) Violin plot of BMI score divided by *SLC7A11* expression. (g) Representative IHC staining figures of *ALOX12*. (h) Representative IHC staining figures of *SLC7A11*.
FUSCC, Fudan University Shanghai Cancer Center; IHC, immunohistochemistry; RFS, recurrence-free survival; TNBC, triple-negative breast cancer.

microenvironment among TNBC, thereby enhancing the effectiveness of immunotherapy associated with its role in iron metabolism and oxidative stress response. These findings suggested that *FTH1* could be a promising biomarker for TNBC immunotherapy.

In conclusion, the present study discovered the prognostic value of ferroptosis-related genes in breast cancer patients and set up a nomogram model. Furthermore, we found *FTH1* as a promising predictor for TNBC immunotherapy.

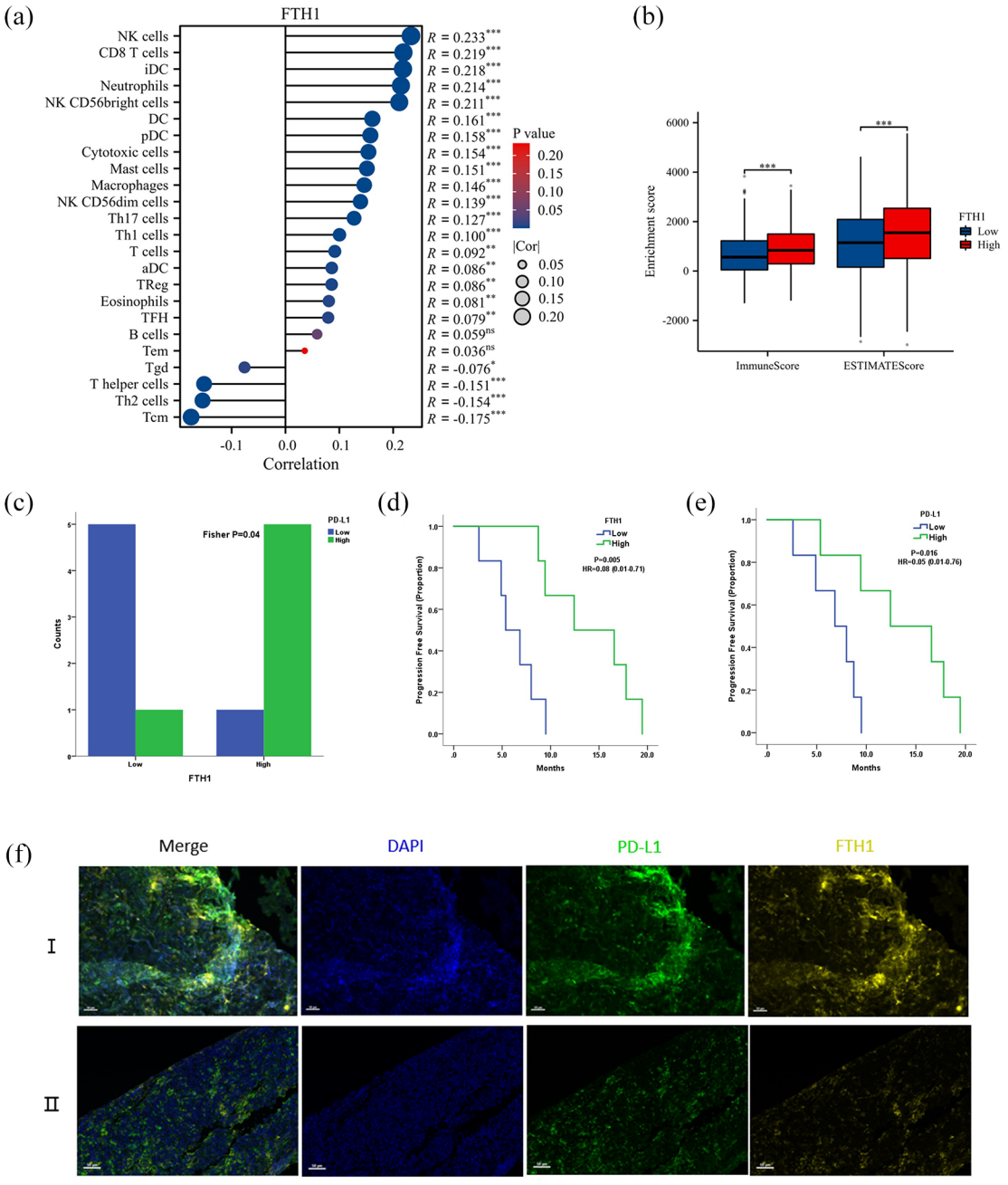

Figure 5. Immunotherapy prediction value of *FTH1*. (a) Immuno-infiltration analysis of TCGA-BRCA database using ssGSEA model. (b) Immuno-infiltration analysis of TCGA-BRCA database using ESTIMATE model. (c) Relationship between *FTH1* expression and PD-L1 expression in TNBC immunotherapy cohort of FUSCC. (d) Kaplan–Meier curves for PFS divided by *FTH1* expression in the FUSCC cohort. (e) Kaplan–Meier curves for PFS divided by PD-L1 expression in the FUSCC cohort. (f) Representative immunotherapy patient immunofluorescence confocal images: Patient I, High expression of *FTH1* and PD-L1, with good response to immunotherapy; Patient II: Low expression of *FTH1* and PD-L1, with poor response to immunotherapy.
FUSCC, Fudan University Shanghai Cancer Center; PD-L1, programmed death ligand 1; TNBC, triple-negative breast cancer.

This study mostly focused on the prognostic and immune-prediction value of ferroptosis-related genes without more fundamental work. Thus, further explorations on the function and potential mechanisms are warranted in the future.

Table 3. Baseline patient characteristics receiving immunotherapy in FUSCC divided by *FTH1* expression.

Characteristics	FTH1 low *N* = 6	FTH1 high *N* = 6	*p* Values
Median age	55	45	0.18
(Range)	(34–69)	(32–57)	
Menopausal status			
Postmenopausal	2	4	0.28
Premenopausal	4	2	
DFI (years)			
<2	5	1	0.04
⩾2	1	5	
ECOG score			
0–1	6	6	1
Number of metastatic sites			
1	2	2	0.48
2	2	0	
⩾3	2	4	
Metastatic sites			
Bone	3	4	0.5
Visceral	5	2	0.24
PD-L1 expression			
High	1	5	0.04
Low	5	1	
IATH			
Low	1	1	1
High	5	5	
IETH			
Low	2	1	0.5
High	4	5	

DFI, Disease-Free Survival; FTH1, Ferritin Heavy Chain 1; FUSCC, Fudan University Shanghai Cancer Center; PD-L1, programmed death ligand 1.

Conclusion

Ferroptosis-related genes like *ALOX12* and *SLC7A11* had potential prognostic value for breast cancer patients. Furthermore, *FTH1* could predict immunotherapy outcomes for TNBC patients.

Declarations

Ethics approval and consent to participate

All procedures performed in studies involving human participants were in accordance with the ethical standards of the institutional research

committee and with the 1964 Helsinki Declaration and its later amendments or comparable ethical standards. The study has been exempted from written informed consent and requires ethics approval from the Institutional Review Board of Fudan University Cancer Hospital as the patient record was retrospectively collected.

Consent for publication
Not applicable.

Author contributions
Yizhao Xie: Data curation; Formal analysis; Writing – original draft.

Zhonghua Tao: Methodology; Writing – original draft.

Biyun Wang: Investigation.

Yannan Zhao: Data curation.

Xinyu Chen: Resources.

Bin Li: Software.

Jinyan Wang: Methodology.

Guangliang Chen: Project administration; Writing – review & editing.

Xichun Hu: Conceptualization; Writing – review & editing.

Acknowledgements
The authors would like to thank lab assistants, teachers, and colleges for their support of this study.

Funding
The author(s) disclosed receipt of the following financial support for the research, authorship, and/or publication of this article: This study was supported by the National Natural Science Foundation of China (82473071 to Xichun Hu), Program for Shanghai Outstanding Academic Leader (LJRC2102, LJRC2102-P), Shanghai Anticancer Association SOAR PROJECT (SACA-AX202402, SACA-AX202106). The funding agencies had no role in study design, data collection, and analysis, decision to publish, or preparation of the manuscript.

Competing interests
The authors declare that there is no conflict of interest.

Availability of data and materials
The datasets collected and/or analyzed during this study are not publicly available due to hospital policies but are available from the corresponding author upon reasonable request.

ORCID iDs
Zhonghua Tao https://orcid.org/0000-0003-3975-3803

Biyun Wang https://orcid.org/0000-0002-7829-1544

Xichun Hu https://orcid.org/0000-0001-6148-9186

Supplemental material
Supplemental material for this article is available online.

References
1. Sung H, Ferlay J, Siegel RL, et al. Global cancer statistics 2020: GLOBOCAN estimates of incidence and mortality worldwide for 36 cancers in 185 countries. *CA Cancer J Clin* 2021; 71(3): 209–249.
2. Perou CM, Sørlie T, Eisen MB, et al. Molecular portraits of human breast tumours. *Nature* 2000; 406(6797): 747–752.
3. Li X, Yang J, Peng L, et al. Triple-negative breast cancer has worse overall survival and cause-specific survival than non-triple-negative breast cancer. *Breast Cancer Res Treat* 2017; 161(2): 279–287.
4. Foulkes WD, Smith IE and Reis-Filho JS. Triple-negative breast cancer. *N Engl J Med* 2010; 363(20): 1938–1948.
5. Chen X, Kang R, Kroemer G, et al. Broadening horizons: the role of ferroptosis in cancer. *Nat Rev Clin Oncol* 2021; 18(5): 280–296.
6. Conrad M and Pratt DA. The chemical basis of ferroptosis. *Nat Chem Biol* 2019; 15(12): 1137–1147.
7. Hong T, Lei G, Chen X, et al. PARP inhibition promotes ferroptosis via repressing SLC7A11 and synergizes with ferroptosis inducers in BRCA-proficient ovarian cancer. *Redox Biol* 2021; 42: 101928.
8. Wang W, Green M, Choi JE, et al. CD8+ T cells regulate tumour ferroptosis during cancer immunotherapy. *Nature* 2019; 569(7755): 270–274.

9. Schmid P, Rugo HS, Adams S, et al. Atezolizumab plus nab-paclitaxel as first-line treatment for unresectable, locally advanced or metastatic triple-negative breast cancer (IMpassion130): updated efficacy results from a randomised, double-blind, placebo-controlled, phase 3 trial. *Lancet Oncol* 2020; 21(1): 44–59.
10. Miles D, Gligorov J, André F, et al. Primary results from IMpassion131, a double-blind, placebo-controlled, randomised phase III trial of first-line paclitaxel with or without atezolizumab for unresectable locally advanced/metastatic triple-negative breast cancer. *Ann Oncol* 2021; 32(8): 994–1004.
11. Cescon DW, Cescon DW, Rugo HS, et al. Pembrolizumab plus chemotherapy versus placebo plus chemotherapy for previously untreated locally recurrent inoperable or metastatic triple-negative breast cancer (KEYNOTE-355): a randomised, placebo-controlled, double-blind, phase 3 clinical trial. *Lancet* 2020; 396(10265): 1817–1828.
12. Wang J, Zhang X, Beck AH, et al. Alcohol consumption and risk of breast cancer by tumor receptor expression. *Horm Cancer* 2015; 6(5–6): 237–246.
13. Zhou N and Bao J. FerrDb: a manually curated resource for regulators and markers of ferroptosis and ferroptosis-disease associations. *Database* 2020; 2020: baaa021.
14. Zhou Y, Zhou B, Pache L, et al. Metascape provides a biologist-oriented resource for the analysis of systems-level datasets. *Nat Commun* 2019; 10(1): 1523.
15. Ferrone CR, Kattan MW, Tomlinson JS, et al. Validation of a postresection pancreatic adenocarcinoma nomogram for disease-specific survival. *J Clin Oncol* 2005; 23(30): 7529–7535.
16. Hanzelmann S, Castelo R and Guinney J. GSVA: gene set variation analysis for microarray and RNA-seq data. *BMC Bioinformatics* 2013; 14: 7.
17. Bindea G, Mlecnik B, Tosolini M, et al. Spatiotemporal dynamics of intratumoral immune cells reveal the immune landscape in human cancer. *Immunity* 2013; 39(4): 782–795.
18. Chen X-Y, Li B, Wang Y, et al. Low level of ARID1A contributes to adaptive immune resistance and sensitizes triple-negative breast cancer to immune checkpoint inhibitors. *Cancer Commun (Lond)* 2023; 43(9): 1003–1026.
19. Moons KG, Altman DG, Reitsma JB, et al. Transparent reporting of a multivariable prediction model for individual prognosis or diagnosis (TRIPOD): explanation and elaboration. *Ann Intern Med* 2015; 162(1): W1–W73.
20. Xie Y, Wang B, Zhao Y, et al. Mammary adipocytes protect triple-negative breast cancer cells from ferroptosis. *J Hematol Oncol* 2022; 15(1): 72.
21. Yang WS, SriRamaratnam R, Welsch ME, et al. Regulation of ferroptotic cancer cell death by GPX4. *Cell* 2014; 156(1–2): 317–331.
22. Ma S, Henson ES, Chen Y, et al. Ferroptosis is induced following siramesine and lapatinib treatment of breast cancer cells. *Cell Death Dis* 2016; 7: e2307.
23. Yu M, Gai C, Li Z, et al. Targeted exosome-encapsulated erastin induced ferroptosis in triple negative breast cancer cells. *Cancer Sci* 2019; 110(10): 3173–3182.
24. Contursi A, Tacconelli S, Hofling U, et al. Biology and pharmacology of platelet-type 12-lipoxygenase in platelets, cancer cells, and their crosstalk. *Biochem Pharmacol* 2022; 205: 115252.
25. Chu B, Kon N, Chen D, et al. ALOX12 is required for p53-mediated tumour suppression through a distinct ferroptosis pathway. *Nat Cell Biol* 2019; 21(5): 579–591.
26. Weng S, Liu Z, Xu H, et al. ALOX12: a novel insight in bevacizumab response, immunotherapy effect, and prognosis of colorectal cancer. *Front Immunol* 2022; 13: 910582.
27. Masaldan S, Bush AI, Devos D, et al. Striking while the iron is hot: iron metabolism and ferroptosis in neurodegeneration. *Free Radic Biol Med* 2019; 133: 221–233.
28. Tian Y, Lu J, Hao X, et al. FTH1 inhibits ferroptosis through ferritinophagy in the 6-OHDA model of Parkinson's disease. *Neurotherapeutics* 2020; 17(4): 1796–1812.
29. Rui T, Wang H, Li Q, et al. Deletion of ferritin H in neurons counteracts the protective effect of melatonin against traumatic brain injury-induced ferroptosis. *J Pineal Res* 2021; 70(2): e12704.